RSC Advances

PAPER

View Article Online
View Journal | View Issue

Cite this: *RSC Adv.*, 2014, **4**, 13481

Zirconium–Beta zeolite as a robust catalyst for the transformation of levulinic acid to γ-valerolactone *via* Meerwein–Ponndorf–Verley reduction†

Jie Wang, Stephan Jaenicke and Gaik-Khuan Chuah*

Received 8th February 2014
Accepted 26th February 2014

DOI: 10.1039/c4ra01120a

www.rsc.org/advances

Zr–Beta zeolite is a robust and active catalyst for the Meerwein–Ponndorf–Verley reduction of levulinic acid to γ-valerolactone, a versatile intermediate for bio-fuels and chemicals. In a batch reactor, γ-valerolactone was formed with a selectivity of >96%. In a continuous flow reactor, >99% yield of γ-valerolactone was obtained with a steady space-time-yield of 0.46 $mol_{GVL}g_{Zr}^{-1}$ h^{-1} within 87 h, on a par with that of noble metal based catalysts. The high activity of this catalyst was attributed to the presence of Lewis acidic sites with moderate strength. Due to the relatively few basic sites, it is not poisoned by the acidic reactant. Its robustness in liquid and gas phase reactants coupled with good thermal stability makes Zr–Beta a green regenerable catalyst that can be used directly on levulinic acid without the need for derivatization.

1 Introduction

The threat of future shortage and ultimately of the depletion of fossil fuels has made the utilization of biomass especially attractive to researchers and manufacturers.[1–5] In a bio-refinery, bio-fuels and value-added chemicals are produced from renewable bio-feedstocks.[6–8] The US Department of Energy has identified several biomass-derived compounds as platform molecules on which to focus future research endeavors.[9,10] Levulinic acid is one of these platform molecules; it can be obtained through hydrolysis/dehydration of hexoses such as glucose and fructose, or hexose-containing polymers like starch and cellulose (Scheme 1).[11–15] The utilization of nonedible lignocelluloses is particularly attractive as it avoids any potential competition with food supplies.[16–18]

The hydrogenation of levulinic acid gives γ-valerolactone (GVL), which is a sustainable liquid for energy and carbon-based chemicals.[19–23] Recently, the group of Dumesic[24] developed a route to convert γ-valerolactone into branched alkanes with molecular weights appropriate for liquid transportation fuels. Esterification of pentenoic acid derived from γ-valerolactone gives "valeric biofuels" which are potential substitutes for gasoline and diesel components.[25] Useful chemicals such as 1,4-pentanediol or 2-methyltetrahydrofuran can be obtained by chemoselective hydrogenolysis of γ-valerolactone.[13,26,27]

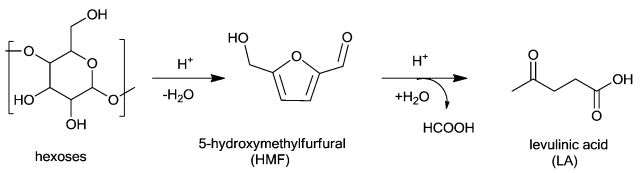

Scheme 1 Catalytic conversion of hexoses into levulinic acid.

As biomass derivatives have high oxygen content, an oxygen removal step is essential for the upgrading of biomass feedstock to biofuels and chemicals.[10,28] This normally requires external H_2 incurring drawbacks such as the need for pressure equipment, the loss of the petroleum-derived H_2 in the form of water, and the use of noble metal-based homogeneous or heterogeneous catalysts.[29–34] Instead of gaseous H_2, the catalytic transfer hydrogenation (CTH) process offers an alternative approach by using hydrogen donors such as formic acid, formate salts, sec-alcohols, cyclohexene and hydrazine.[35] The use of formic acid for reduction is especially attractive since an equimolar amount of formic acid is formed during the production of levulinic acid from carbohydrates.[36–39] However, the reaction requires expensive noble metal catalysts[36–38] or harsh conditions.[39,40] Furthermore, the noble metals catalyze the decomposition of formic acid so that the reduction seems to proceed *via in situ* formed H_2 rather than transfer hydrogenation, necessitating the use of a closed system.[36–38]

Instead of formic acid, the carbonyl group in levulinic acid can be reduced by secondary alcohols *via* the Meerwein–Ponndorf–Verley (MPV)[41–43] reduction (Scheme 2). Wise and Williams[44] showed that although the carbonyl group of levulinic acid is not chemically labile, the reaction is favored due to lactonisation of 4-hydroxypentanoic acid (4-HPA) to

Department of Chemistry, National University of Singapore, 3 Science Drive 3, Kent Ridge, 117543, Singapore. E-mail: chmcgk@nus.edu.sg; Fax: +65 6779 1691; Tel: +65 6516 2839

† Electronic supplementary information (ESI) available: Fig. S1–S10, Tables S1 and S2. See DOI: 10.1039/c4ra01120a

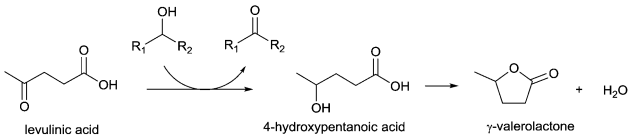

Scheme 2 MPV reduction of levulinic acid to γ-valerolactone.

γ-valerolactone. However, little attention was paid to this strategy, until Chia and Dumesic[45] recently screened different metal oxides for this reaction and found that zirconium oxide was the most active. In the flow sheet of the bio-refinery, the biomass is primarily transferred into 5-hydromethylfurfural (HMF) which further hydrolyses to levulinic acid.[46] Following this, a biphasic system could be employed to extract the levulinic acid from the aqueous phase.[47,48] If sec-alcohols are employed as the extraction reagent, they can form alternative hydrogen donors other than formic acid. The MPV reaction has the advantage that inexpensive non-noble metal catalysts can be used. Whilst the traditional MPV catalyst was aluminium alkoxide, a number of heterogeneous catalysts such as zeolites,[49–52] mesoporous materials,[53,54] metal oxides or hydroxides,[55–62] hydrotalcites[63,64] and K_3PO_4 (ref. 65) have been reported in recent times. The conditions for liquid phase MPV reduction are usually mild, taking place under ambient pressure at the boiling point of the secondary alcohol.

Our previous work has shown that zirconium-based catalysts, especially Zr–Beta zeolites, are highly active for the MPV reduction of substituted cyclohexanones and α,β-unsaturated aldehydes.[52,66,67] This motivated us to investigate the use of Zr-Beta in the MPV reduction of levulinic acid to γ-valerolactone. By incorporating very small amounts of zirconium (Si/Zr ~75–200) into the zeolite framework, isolated zirconium atoms with Lewis acidic property are formed. Computational studies using density functional theory show that the zirconium ions are located at specific crystallographic positions of the zeolite framework and play an important role in adsorption and activation of reactants.[68] The ability of the catalyst to function under acidic conditions is important for the title reaction. Hydrous zirconia ($ZrO(OH)_n$) and zirconia (ZrO_2) have been compared. The activities were tested in a batch reactor as well as in a continuous flow reactor for potential industrial utilization.

2 Experimental

2.1 Catalyst preparation

Synthesis of Zr–Beta and ZrAl–Beta zeolites. Zr–Beta zeolites (Si/Zr 75, 100, 150, 200) were synthesized in fluoride medium following the procedure reported previously.[52] Briefly, 10.42 g TEOS was mixed with 10.31 g tetraethyl-ammonium hydroxide (TEAOH, 40 wt% solution) and hydrolyzed under stirring. After 2 h, 1.55 g of an aqueous solution containing the required amount of $ZrOCl_2 \cdot 8H_2O$ was added dropwise. The mixture was stirred for another 7–8 h until the ethanol formed upon hydrolysis of TEOS was evaporated. Finally, 1.215 ml of HF (40% solution) and 0.105 g pure silica zeolite Beta seeds in 1 g of water were sequentially added. The crystallization was carried out in a Teflon-lined stainless steel autoclave at 140 °C for 20 days. The solid product obtained was filtered, washed with deionized water, dried at 100 °C and calcined at 580 °C for 10 h. ZrAl–Beta zeolites were synthesized following the above procedure with 0.161 g $ZrOCl_2 \cdot 8H_2O$ (Si/Zr 100) and varying amounts of $Al(NO_3)_3 \cdot 9H_2O$. The samples are denoted as Zr-Beta-*x* or ZrAl-Beta-*y*, where *x* and *y* stands for the Si/Zr and Si/Al ratio, respectively.

Synthesis of hydrous zirconia and zirconium oxide. A 10 wt% aqueous solution of $ZrCl_4$ was added dropwise into an excess of 5 M ammonium hydroxide solution. After aging for 24 h, the suspension was digested in a Teflon round-bottom flask at 100 °C for another 48 h, filtered and the precipitate washed free of chloride. The as-synthesized hydrous zirconia, $ZrO(OH)_n$-100, was dried overnight at 100 °C. Hydrous zirconia calcined at different temperatures for 2 h are designated as $ZrO(OH)_n$-*T*, where *T* stands for the temperature of calcination (°C).

2.2 Characterization

The surface area and porosity of the samples were determined by nitrogen adsorption (Micromeritics Tristar 3000). Prior to each measurement, the sample was thoroughly degassed under a nitrogen flow for 4 h. The degassing temperature was 100 °C for $ZrO(OH)_n$ calcined below 300 °C, and 300 °C for the other catalysts. The crystalline phase was determined by powder X-ray diffraction (Siemens D5005 equipped with Cu anode and variable slits). The diffractograms were measured at a step size of 0.02° and a dwell time of 1 s. The elemental composition was determined by inductively coupled plasma-atomic emission spectroscopy (ICP-AES) after dissolving the sample in HF. Infrared spectra of the samples in KBr were recorded in the range of 4000–400 cm^{-1} using a Bio-Rad Excalibur FT-IR spectrometer with a resolution of 4 cm^{-1}. Thermogravimetric analyses were performed on a Dupont SDT 2960 apparatus to determine the water content in the hydrous zirconia. The sample was kept at 100 °C for 0.5 h to remove physically absorbed water, and then heated to 800 °C at 10 °C min^{-1}. The degree of hydroxylation was calculated from the weight loss. The desorption of residual organics on used Zr-Beta as well as the catalyst with adsorbed levulinic acid or γ-valerolactone was measured by thermogravimetry combined with mass spectrometry (Mettler-Toledo TGA/DSC Star^e with Pfeiffer Thermostar mass spectrometer). The acidic and basic nature of the samples was quantified by temperature programmed desorption of NH_3 and CO_2, respectively. The sample was pretreated at its calcined temperature for 2 h in a flow of helium (50 ml min^{-1}). After cooling to 100 °C, NH_3 or CO_2 gas was introduced for 15 min. The sample was flushed with helium for another 2 h before heating at 10 °C min^{-1}. The desorption of NH_3 or CO_2 was monitored by a quadrupole mass spectrometer (Balzers Prisma 200). Lewis and Brønsted acidity was investigated by FT-IR spectra of adsorbed pyridine. A self-supporting sample disc (10–20 mg) was pretreated in an evacuated (100 Pa) glass cell at 300 °C for 2 h. After cooling to room temperature, a background spectrum was recorded using a Bio-Rad Excalibur FT-IR spectrometer. The sample was exposed to pyridine for 15 min and re-evacuated at 100–300 °C for 1 h before measuring the IR spectra.

2.3 Catalytic activity evaluation

Batch reaction. Typically, a reaction mixture containing 1 mmol levulinic acid and 5 ml sec-alcohol as solvent and hydrogen donor was placed in a 25 ml round-bottomed flask equipped with a septum port, reflux condenser and a guard tube. *N*-dodecane was added as internal standard to monitor the mass balance during the reaction. After heating to the desired temperature, 100 or 200 mg of catalyst was added to the reaction mixture. Aliquots were removed at different reaction times and the products were analyzed by gas chromatography (GC) and gas chromatography mass spectrometry (GCMS). For temperatures higher than the boiling point of the alcohol, the reaction was carried out under He (5 bar) in a 50 ml Teflon-lined autoclave (Parr) equipped with magnetic stirring.

Continuous flow reaction. The catalyst bed of Zr-Beta-100 catalyst (200 or 500 mg depending on the required space velocity) and glass beads (701-1, 180 microns, Sigma-Aldrich) was placed on a fritted disk in a quartz reactor (i.d. 10 mm). The temperature of the reactor was controlled by a Eurotherm temperature controller. The liquid feed containing 5 wt% levulinic acid in 2-propanol was introduced into the reactor with co-feeding of He in a downflow configuration. The liquid feed rate was varied using a syringe pump (New Era, NE-1000). The He flow rate of 20 ml min^{-1} was controlled by a mass flow controller (Brooks 5850). The eluent was condensed in an ice-cooled trap and samples were taken periodically for GC analysis. For regeneration, the catalyst was calcined *in situ* at 500 °C under a flow of air (50 ml min^{-1}) for 3 h.

Sample analysis. The collected samples were analyzed on a gas chromatograph (HP 6890) equipped with a HP-FFAP capillary column (250 μm × 0.25 μm × 30 m) and a flame ionization detector. The products were verified either by comparing the retention times with authentic samples or by GCMS analysis. Mass balances closed within 5% for all data points.

3 Results and discussion

3.1 Materials

The X-ray diffractograms of Zr-Beta samples (Si/Zr 75–200) showed the characteristic peaks of the zeolite Beta phase

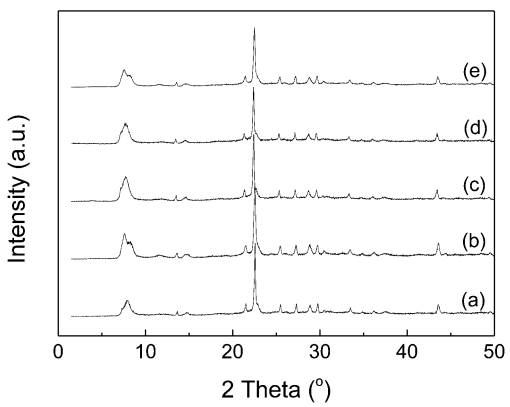

Fig. 1 X-ray diffraction patterns of (a) Zr-Beta-75 (b) Zr-Beta-100 (c) Zr-Beta-150 (d) Zr-Beta-200 and (e) ZrAl-Beta-100.

Table 1 Textural properties of (Zr, Al)–Beta zeolites

Sample	Si/Zr[a]	Si/Al[a]	BET surf. area (m^2 g^{-1})	Pore vol. (cm^3 g^{-1})
Zr-Beta-75	78	—	503	0.29
Zr-Beta-100	107	—	474	0.27
Zr-Beta-150	163	—	439	0.27
Zr-Beta-200	209	—	436	0.26
ZrAl-Beta-25	105	27	490	0.27
ZrAl-Beta-100	110	104	454	0.26

[a] Determined by ICP analyses.

(Fig. 1). The samples had high surface areas between 436–503 m^2 g^{-1}. The ZrAl-Beta samples showed similar textural properties as the Zr–Beta zeolites (Table 1). All the samples were largely microporous with total pore volumes of 0.26–0.29 cm^3 g^{-1}. The ICP analyses confirmed that both aluminium and zirconium were successfully incorporated into the samples, although the Si/Al and Si/Zr ratios in the zeolite were slightly higher than in the initial synthesis gel.

The as-synthesized hydrous zirconia dried at 100 °C had a high surface area of 400 m^2 g^{-1} (Table 2) and contained micropores as well as mesopores up to 12 nm (Fig. S1†). After calcination at 300 °C, the surface area was reduced to 271 m^2 g^{-1}. Although there was a reduction in the micropore volume, the pore size distribution of the mesopores remained similar to that of the as-synthesized sample. However, after calcination at 400 and 600 °C, the surface area decreased to 141 and 51 m^2 g^{-1}, respectively. The samples calcined above 400 °C contained bigger mesopores in the range of 8–20 nm. XRD showed that the hydrous zirconia samples were amorphous, but after calcination at 400 °C, crystalline zirconia with predominantly monoclinic phase was formed (Fig. S2†). The percentage of monoclinic phase increased from 77 to 83% as the calcination temperature was raised from 400 to 600 °C. The transformation to zirconia is accompanied by condensation of the hydroxyl groups in hydrous zirconia and the weight loss was monitored by thermogravimetry. Samples calcined at higher temperatures had smaller weight loss.

The amount of water, *n*, associated with the hydrous zirconia, $ZrO_2 \cdot nH_2O$, decreased from 0.92 in the as-synthesized

Table 2 Textural properties of hydrous zirconia and zirconia

Sample	Surf. area (m^2 g^{-1})	Mean pore[a] ϕ (nm)	Pore vol. (cm^3 g^{-1})	Monoclinic phase (%)	Weight loss[b] (%)
$ZrO(OH)_n$-100	400	5.3	0.56	Amorp.	11.8
$ZrO(OH)_n$-200	326	5.3	0.47	Amorp.	8.3
$ZrO(OH)_n$-300	271	5.5	0.42	Amorp.	7.1
$ZrO(OH)_n$-400	141	8.4	0.35	77	4.2
$ZrO(OH)_n$-500	84	12.5	0.32	81	3.8
$ZrO(OH)_n$-600	51	17.0	0.26	83	3.6

[a] Pore size distributions were calculated from the desorption branch of the isotherms by the BJH method. [b] From TGA results in the range of 100 to 800 °C.

Table 3 Acid–base properties of the catalysts

Sample	Acidity[a] (μmol g^{-1}) Weak	Strong	L/B ratio[b]	Basicity (μmol g^{-1})
$ZrO(OH)_n$-300	137	—	6.7	132
$ZrO(OH)_n$-400	99	204	2.1	112
$ZrO(OH)_n$-500	25	146	n.d	53
$ZrO(OH)_n$-600	12	35	n.d	25
Zr-Beta-100	45 (In total)		8.4	3.8
ZrAl-Beta-25	n.d.		0.85	n.d

[a] Integrated from the NH_3 TPD peak areas with cutoff at ~300 °C. [b] Lewis/Brønsted ratio from pyridine IR after heating at 100 °C for 1 h.

sample to 0.30 after calcination at 400 °C. These results correlate well with that from IR spectroscopy (Fig. S3†). Hydrous zirconia has absorption bands at *ca.* 3400 cm^{-1} due to O–H stretching, *ca.* 1620 cm^{-1} due to the scissor bending mode of coordinated molecular water and *ca.* 1390 cm^{-1} due to atmospheric CO_2 adsorbed on the sample forming a bicarbonate-like species.[69,70] All these bands decreased in intensity as the sample was heated to higher temperatures.

The overall acidity and basicity of the samples was determined by TPD of NH_3 and CO_2, respectively (Table 3). For $ZrO(OH)_n$-300, desorption of NH_3 was observed from 120 to 300 °C with a maximum at 200 °C (Fig. 2). When hydrous zirconia had been calcined to 400 °C and higher, the NH_3 desorption curve became bimodal with maxima at around 200 °C and 420 °C. The lower temperature peak below 300 °C was assigned to desorption from weak acid sites while NH_3 desorption above this temperature was taken to be indicative of strong acidic sites. After calcination at 400 °C, the amorphous hydrous zirconia transformed to crystalline zirconia. The results show that the resulting oxide has weak as well as strong acid sites, with the latter being predominant. The density of both weak and strong acid sites decreased with higher calcination temperature, due to a loss in surface area. In contrast to hydrous zirconia, Zr-Beta-100 has acid sites of moderate strength. The NH_3 desorption occurred between 220 to 390 °C, which is in the temperature range intermediate between the low and temperature peaks observed for hydrous zirconia. Furthermore, the density of acidic sites, 45 μmol g^{-1}, was lower than that for the zirconia samples.

The nature of the acid sites on the catalysts was determined by FT-IR measurements after adsorption of pyridine (Fig. S4† and Table 3). The bands at 1446 and 1540 cm^{-1} are assigned to pyridine adsorbed at Lewis and Brønsted acid sites, respectively.[71] On $ZrO(OH)_n$-300 and Zr-Beta-100, Lewis acid sites dominated, with Lewis/Brønsted ratio of 6.7 and 8.4, respectively. Only weak Brønsted acid sites were found for these two samples as the intensity of the 1540 cm^{-1} band decreased significantly after heating at 100 °C. On the other hand, $ZrO(OH)_n$-400 and ZrAl-Beta-25 showed stronger Brønsted acid sites as the 1540 cm^{-1} band was still present even after heating to 200 °C. These samples had a higher density of Brønsted acid sites than Zr-Beta-100.

The presence of basic sites was probed by CO_2 TPD. There was hardly any desorption of CO_2 from Zr-Beta-100 showing that it has very few basic sites. In contrast, the amount of CO_2 desorbed from hydrous zirconia/zirconia was in the range of 25 to 132 μmol g^{-1}, reflecting the amphoteric nature of these samples. With increase of calcination temperature from 300 to 600 °C, the CO_2 desorption was shifted to higher temperatures, indicating an increase in the basicity of the samples (Fig. S5†).

3.2 Effect of sec-alcohol and reaction temperature

The MPV reduction of levulinic acid was tested using a number of different secondary alcohols. The alcohols were used in excess, acting both as solvent and as hydrogen donor. Normally, 2-propanol is the best reducing agent.[52,65] However, in the liquid phase reduction of levulinic acid with 2-propanol, only 5.6% conversion was obtained after 18 h despite using 200 mg of Zr-Beta-100 (Table 4). The low activity could be due to the aliphatic nature of levulinic acid as Zr-Beta had previously been shown to be a highly efficient catalyst for the MPV reduction of cyclohexanones and α,β-unsaturated aldehydes.[52] The formation of γ-valerolactone involves the tandem reduction of levulinic acid to 4-hydroxypentanoic acid followed by cyclization and loss of one molecule of water. By using 2-propanol as the hydrogen donor and solvent, the reaction temperature is limited to 82 °C

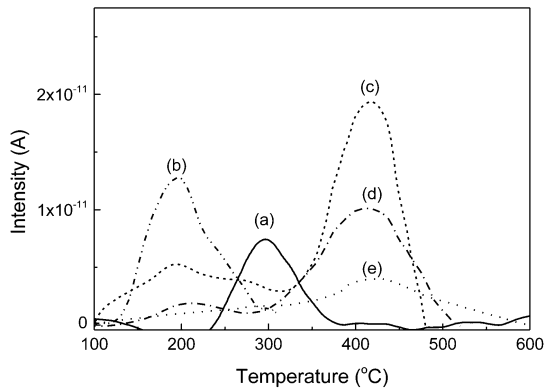

Fig. 2 NH_3 desorption profiles of (a) Zr-Beta-100 (b) $ZrO(OH)_n$-300 (c) $ZrO(OH)_n$-400 (d) $ZrO(OH)_n$-500 and (e) $ZrO(OH)_n$-600.

Table 4 MPV reduction of levulinic acid using different sec-alcohols over Zr-Beta-100[a]

Alcohol	Temp. (°C)	Time (h)	LA conv. (%)	GVL sel. (%)	GVL yield (%)
2-propanol	82	18	5.6	72	4.0
2-butanol	100	18	77	93	72
2-pentanol	100	18	58	95	55
2-pentanol	118	10	100	96	96
2-pentanol	118	22[b]	88	95	83
Cyclohexanol	150	6	100[c]	82	82

[a] Reaction condition: 200 mg Zr-Beta-100, 1 mmol LA, 5 ml sec-alcohol. [b] 100 mg Zr-Beta-100 as the catalyst. [c] By-products from cyclohexanol were formed.

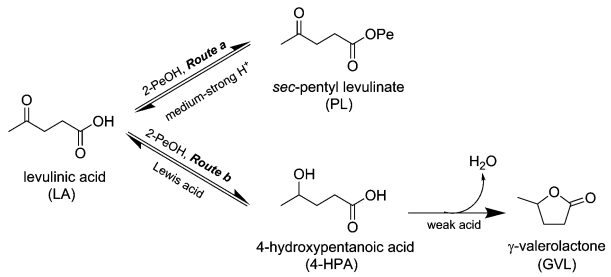

Scheme 3 Transformation of levulinic acid to γ-valerolactone and ester.

in open system which may be too low to remove the water formed. To increase the reaction temperature, aliphatic secondary alcohols with higher boiling points like 2-butanol and 2-pentanol were employed.

The conversion increased significantly to 77% when using 2-butanol at 100 °C. Although the reducing capability of 2-pentanol is not as good as that of 2-butanol, giving only 58% conversion of levulinic acid at 100 °C, its higher boiling point of 118 °C enabled a faster MPV reduction in liquid phase. Hence, after 10 h, full conversion was achieved. For all these linear alcohols, the only by-product was due to esterification between levulinic acid and the corresponding alcohol. Cyclohexanol has an even higher boiling point, but by-products such as cyclohexene were formed when the reaction was conducted at 150 °C.

3.3 Effect of substrate concentration

The sec-alcohol was used in excess (46 equiv.) and served both as the solvent and reducing agent. As levulinic acid has both carbonyl and carboxyl groups, two competing reactions, MPV reduction and esterification, can occur simultaneously (Scheme 3). An increase in the concentration of the limiting substrate accelerates both reactions. However, at higher concentrations of levulinic acid, the selectivity to γ-valerolactone was lower, showing that the esterification rate increased more than the MPV reduction. Use of 2 ml of 2-pentanol (7.2 wt% levulinic acid) resulted in only 75% selectivity to γ-valerolactone at full conversion whereas with 5 ml of 2-pentanol (2.9 wt% levulinic acid), 98% selectivity with 46% conversion was observed after 6 h (Table S1†). Even without adding any catalyst, the yield of the ester increased with higher levulinic acid concentration (Table S2†). Hence, a dilute system of 1 mmol (2.9 wt%) levulinic acid in 5 ml solvent was employed in the liquid phase to eliminate to reduce the rate of esterification and improve the selectivity to γ-valerolactone.

3.4 Catalyst screening for liquid phase transformation

Comparing the Zr–Beta zeolites with different Si/Zr ratios, Zr-Beta-100 showed the best activity with 100% conversion and a very high selectivity of 96% to γ-valerolactone (Table 5). The only by-product was sec-pentyl levulinate due to esterification. Over Zr-Beta-150 and Zr-Beta-200, the conversion was lower, 71% and 27%, respectively. This may be attributed to the lower zirconium content in these samples. Despite their lower activity, the selectivity to γ-valerolactone was high, between 97–99%. On the other hand, Zr-Beta-75 contained more zirconium than Zr-Beta-100 but this catalyst was less active and selective, suggesting that an optimum number of isolated zirconium sites is essential for reaction. Based on the levulinic acid converted per g of Zr, the initial rates of the Zr-Beta catalysts with Si/Zr of 75–200 was between 16–31 $mmol_{GVL}g_{Zr}^{-1}$ h^{-1}. The low initial rate indicates the difficulty to reduce the aliphatic carbonyl group in levulinic acid. In comparison, the initial rate for the MPV reduction of cyclohexanone and α,β-unsaturated aldehydes,[52] is generally 20–30 times larger even at a lower temperature of 82 °C. To check for any leaching, the Zr-Beta-100 was hot filtered from the reaction medium after the conversion had reached 40%. No further increase in conversion was observed in the

Table 5 MPV reduction of levulinic acid over zirconium-based catalysts[a]

Catalyst	Time (h)	LA conv. (%)	GVL sel. (%)	GVL yield (%)	Initial rate[c] ($mmol_{GVL}g_{Zr}^{-1}$ h^{-1})
Zr-Beta-75	10	88	93	82	19
Zr-Beta-100	10	100	96	96	30
Zr-Beta-150	10	71	97	69	31
Zr-Beta-200	10	27	>99	27	16
ZrAl-Beta-25	6	100	71	71	—
ZrAl-Beta-100	6	91	79	72	—
$ZrO(OH)_n$-100	24	11	74	8.3	0.071
$ZrO(OH)_n$-200	24	13	67	8.8	0.075
$ZrO(OH)_n$-300	24	16	67	11	0.096
$ZrO(OH)_n$-400	24	37	62	23	0.22
$ZrO(OH)_n$-500	24	33	33	11	0.16
$ZrO(OH)_n$-600	24	12	45	5.4	0.076
Zr-Beta-100	6	100[b]	92	92	—
$ZrO(OH)_n$-200	16	68[b]	56	38	—
$ZrO(OH)_n$-400	16	89[b]	46	41	—
$ZrO(OH)_n$-600	16	45[b]	36	16	—

[a] Reaction conditions: 200 mg catalyst, 1 mmol LA, 5 ml 2-pentanol, 118 °C, reflux. [b] Reaction conditions: 100 mg catalyst, 2 mmol LA, 5 ml 2-butanol, 150 °C and autogenous pressure plus 5 bar He in autoclave. [c] Calculated based on the conversion after first 2 h.

catalyst-free reaction mixture, showing that the MPV reduction of levulinic acid is heterogeneously catalyzed by Zr-Beta.

The incorporation of Al into Zr-Beta led to Brønsted acidity which promoted the conversion of levulinic acid. Over ZrAl-Beta-25, the time for full conversion was reduced from 10 h to 6 h. However, the presence of strong Brønsted acid sites accelerated the esterification to sec-pentyl levulinate so that at 100% conversion, the selectivity to γ-valerolactone was only 71% (Scheme 3, Route a). Furthermore, the Brønsted acid sites catalyzed other side reactions of pentanol leading to hemiacetals, pentene and its isomers. Hence, the MPV reduction of the carbonyl group in levulinic acid is best catalyzed by a Lewis acid catalyst as the presence of Brønsted acid sites will reduce the overall selectivity to γ-valerolactone.

Compared to Zr-Beta zeolites, the $ZrO(OH)_n$-*T* samples were less active and selective. After 24 h, the conversion was only between 11 to 37% (Table 5). The selectivity to γ-valerolactone decreased from 74 to 45% with increasing calcination temperature of the hydrous zirconia. The best catalyst among the hydrous zirconia was $ZrO(OH)_n$-400 with 23% yield of γ-valerolactone. The dependence of the catalytic activity and selectivity on the calcination temperature may be attributed to its effect on the density of surface hydroxyl groups and the acidity of the samples. Surface hydroxyl groups are important in the MPV reaction as they react with the reducing alcohol to form the alkoxide intermediate.[55] With increase of calcination temperature, the density of hydroxyl groups decreased as they condensed to form the oxide. On the other hand, NH_3 TPD results show that stronger acid sites are formed that would favor the cyclization step. Hence a balance in the density of surface hydroxyls and acid strength is important for activity of the hydrous zirconia.

The activity of hydrous zirconia and Zr-Beta-100 were next tested under conditions similar to those reported by Chia and Dumesic.[45] The authors used a closed system at a higher temperature of 150 °C with 2-butanol as the reducing alcohol (Table 5). It was found that a high γ-valerolactone yield of 92% could be achieved based on the zirconium oxide catalyst. However, an extremely dilute system (1 wt% levulinic acid) was necessary. When the concentration was increased to 5 wt%, the selectivity was only 42% at 51% conversion, giving a γ-valerolactone yield of 22% These results are comparable with this work where 16% yield of γ-valerolactone was obtained over $ZrO(OH)_n$-600 (Table 5). We observed that hydrous zirconia calcined at a lower temperature of 400 °C instead of 600 °C, $ZrO(OH)_n$-400, was more active with 89% conversion and 46% yield of γ-valerolactone. Compared to hydrous zirconia, Zr-Beta-100 was able to maintain a very high γ-valerolactone selectivity of 92% at full conversion even at 5 wt% levulinic acid (Table 5).

The better activity of Zr–Beta zeolite for transforming levulinic acid to γ-valerolactone can be attributed to its Lewis acidity of moderate strength and its lack of basic sites which otherwise would react with the carboxylic acid functional group in the substrate. Chia and Dumesic[45] found that levulinic acid was less readily reduced than levulinate esters over zirconia. They suggested that this was due to strong binding of levulinic acid to the basic sites on zirconia, leading to blockage and loss of activity. As Zr-Beta has very few basic sites, such inhibitory effects cannot occur. Furthermore, the microporous structure of the zeolite coupled with the absence of strong acid sites hinder the competing esterification reaction, so that a very high γ-valerolactone selectivity of 93–99% could be obtained.

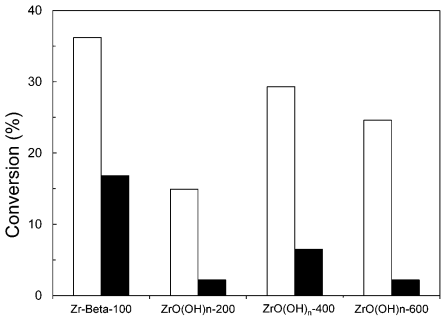

Fig. 3 MPV conversion after 2 h starting from methyl levulinate (□) and levulinic acid (■) over Zr-Beta-100 and $ZrO(OH)_n$-*T*. Reaction conditions: 1 mmol substrate, 5 ml 2-pentanol, 200 mg catalyst, 118 °C.

The influence of the acid group in levulinic acid was investigated by using methyl levulinate as substrate. Over Zr-Beta-100, the conversion after 2 h was about twice that of levulinic acid (Fig. 3). The higher rate of reaction may be explained by the higher hydrophobicity of methyl levulinate which leads to improved adsorption at the surface of the hydrophobic Zr-Beta. The effect was more pronounced over hydrous zirconia where the 2 h-conversion of methyl levulinate was 4.5–11 times higher than levulinic acid. As with levulinic acid, the most active hydrous zirconia sample was $ZrO(OH)_n$-400 with 100% conversion of methyl levulinate after only 6 h.

3.5 Continuous flow reactions over Zr–Beta zeolite

Zr-Beta-100 catalyst was also used in a continuous flow reactor to explore its stability, reusability and potential for industrial application. The feed was 5 wt% levulinic acid in 2-propanol. Initial tests showed that at a reaction temperature of 150 °C with a weight hourly space velocity (WHSV) of 0.16 h^{-1}, full conversion was sustained for around 10 h (Fig. S6†). Due to the high

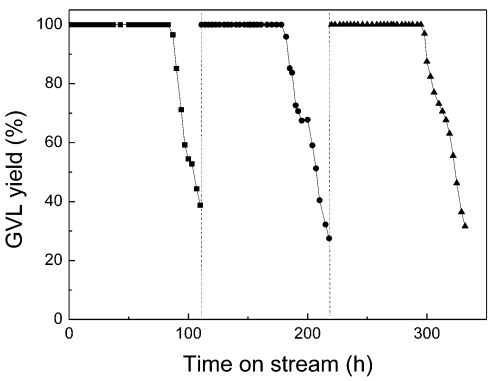

Fig. 4 GVL yield as a function of time on stream for the MPV of levulinic acid over Zr-Beta-100 at 250 °C in a continuous flow reactor of WHSV = 0.64 h^{-1}. Catalyst was regenerated at 110 h and 218 h.

Table 6 Comparison of activity for vapour phase GVL production over different catalysts

Catalyst	T (°C)	P (bar)	H_2 Source[a]	GVL yield (%)	Productivity ($mol_{GVL}g_{metal}^{-1}$ h^{-1})	Stability (h)	Ref.
Zr-Beta	250	1	2-PrOH	>99	0.46	87	—
Ru/C	265	1	H_2	99	0.09	50	74
RuSn/C	220	35	H_2	93	0.36	<100	75
Pd/C + Ru/C	170	35	HCOOBu	95	0.11	400	76
Cu/SiO_2	265	10	H_2	>99	0.09	100	26
ZrO_2	150	20	2-BuOH	20–40	<0.001	150	45

[a] 2-PrOH: 2-propanol; HCOOBu: butyl formate; 2-BuOH: 2-butanol.

boiling points of levulinic acid (245–246 °C) and γ-valerolactone (207–208 °C), it is highly probable that at this low temperature, these molecules remained significantly adsorbed at the surface of the catalyst. Thermogravimetric measurements of Zr-Beta-100 that had been used in the reaction for 34 h showed a weight loss of 9.7% after heating in air to 500 °C (Fig. S7†). The weight loss profile of the used Zr-Beta was similar to that of the catalyst adsorbed with levulinic acid with a steep weight loss between 200 to 350 °C (Fig. S8†). The hydrogen/carbon (H/C) ratio of the used Zr-Beta was 1.57, which is close to the H/C ratio of levulinic acid and γ-valerolactone rather than that of coke in zeolites (H/C around 1.25).[72,73] The catalytic activity was recovered after calcination which also shows that the deactivation was mainly due to the adsorption of substrate and product molecules rather than by heavy coke formation.

To promote the desorption of molecules, the reaction temperature was raised to 250 °C, which is higher than the boiling points, and the space velocity was also increased. At WHSV of 0.64 h^{-1}, the γ-valerolactone yield remained at > 99% for as long as 87 h (Fig. 4). After this time, the conversion dropped and increasing amounts of propyl levulinate were formed. However, the activity was fully regained by recalcining the catalyst in air at 500 °C. Full conversion could again be maintained for prolonged periods of 72 and 78 h in the second and third run, respectively. The stability of the catalyst is of significant importance for industrial applications. The productivity of >99% γ-valerolactone yield under WHSV of 0.64 h^{-1} for the long period works out to 0.46 $mol_{GVL}g_{Zr}^{-1}$ h^{-1}. Pure γ-valerolactone could be obtained by simply distilling off the solvent 2-propanol for reuse in subsequent cycles. The isolated yield was about 93% and the product collected was in high purity as confirmed by ^1H and ^{13}C NMR (Fig. S9†).

At higher space velocities of 2–4 h^{-1}, the average rate of γ-valerolactone formation was around 0.68–0.71 $mol_{GVL}g_{Zr}^{-1}$ h^{-1} (5.7 $mol_{GVL}g_{Zr}^{-1}$ h^{-1} for the first 15 min with WHSV of 4.0 h^{-1}) (Fig. S10†). The sustained productivity using Zr-Beta-100 compares very well with the reported values for metal-based catalysts in vapour phase where the productivity ranges from 0.09 to 0.36 $mol_{GVL}g_{metal}^{-1}$ h^{-1} (Table 6). Due to its high activity for MPV reduction, Zr-Beta offers an alternative to γ-valerolactone formation from levulinic acid without the need for hydrogenation using precious metal catalysts. Furthermore, the reaction can be carried out without the need for high pressure of H_2.

4 Conclusions

Using sec-alcohol as the hydrogen source, biomass-derived levulinic acid was converted to γ-valerolactone *via* a tandem MPV reduction and cyclisation/lactonization. Zr–Beta zeolite (Si/Zr 100) is highly active and selective for the γ-valerolactone production, both in liquid phase batch reactions and in a gas phase continuous flow system. Quantitative conversion with >99% yield of γ-valerolactone was obtained with a steady generation rate of 0.46 $mol_{GVL}g_{Zr}^{-1}$ h^{-1} during a single run in the flow reactor. The presence of Lewis acid sites with moderate strength and only relatively few basic sites are key factors for its good activity and lack of poisoning by the acidic substrate. Due to its high thermal stability, Zr-Beta could be easily recalcined and reused. In comparison, hydrous zirconia and zirconia were less active for the MPV reduction of levulinic acid with the most active hydrous zirconia catalyst being that obtained after calcination at 400 °C.

Acknowledgements

Financial support for this work from the National University of Singapore grants R-143-000-476-112 and R-143-000-550-112 is gratefully acknowledged.

Notes and references

1 G. W. Huber, S. Iborra and A. Corma, *Chem. Rev.*, 2006, **106**, 4044–4098.
2 A. Corma, S. Iborra and A. Velty, *Chem. Rev.*, 2007, **107**, 2411–2502.
3 M. J. Climent, A. Corma and S. Iborra, *Green Chem.*, 2011, **13**, 520–540.
4 J. A. Melero, J. Iglesias and A. Garcia, *Energy Environ. Sci.*, 2012, **5**, 7393–7420.
5 P. Gallezot, *Chem. Soc. Rev.*, 2012, **41**, 1538–1558.
6 B. Kamm, M. Kamm, P. R. Gruber and S. Kromus, in *Biorefineries Industrial Processes and Products: Status Quo and Future Directions*, ed. B.Kamm, P. R. Gruber and M. Kamm, Wiley-VCH, Weinheim, 2006, vol. 1, pp. 3–40.
7 J. H. Clark, V. Budarin, F. E. Deswarte, J. J. Hardy, F. M. Kerton, A. J. Hunt, R. Luque, D. J. Macquarrie, K. Milkowski and A. Rodriguez, *Green Chem.*, 2006, **8**, 853–860.

8 J. H. Clark, F. E. I. Deswarte and T. J. Farmer, *Biofuels, Bioprod. Biorefin.*, 2009, **3**, 72–90.
9 J. J. Bozell and G. R. Petersen, *Green Chem.*, 2010, **12**, 539–554.
10 J. C. Serrano-Ruiz, R. Luque and A. Sepúlveda-Escribano, *Chem. Soc. Rev.*, 2011, **40**, 5266–5281.
11 S. W. Fitzpatrick, *US Pat.*, 5608105, 1997.
12 J. J. Bozell, L. Moens, D. Elliott, Y. Wang, G. Neuenscwander, S. Fitzpatrick, R. Bilski and J. Jarnefeld, *Resour., Conserv. Recycl.*, 2000, **28**, 227–239.
13 H. Mehdi, V. Fábos, R. Tuba, A. Bodor, L. T. Mika and I. T. Horváth, *Top. Catal.*, 2008, **48**, 49–54.
14 O. O. James, S. Maity, L. A. Usman, K. O. Ajanaku, O. O. Ajani, T. O. Siyanbola, S. Sahu and R. Chaubey, *Energy Environ. Sci.*, 2010, **3**, 1833–1850.
15 R. Weingarten, W. C. Conner and G. W. Huber, *Energy Environ. Sci.*, 2012, **5**, 7559–7574.
16 R. Palkovits, *Angew. Chem., Int. Ed.*, 2010, **49**, 4336–4338.
17 D. W. Rackemann and W. O. S. Doherty, *Biofuels, Bioprod. Biorefin.*, 2011, **5**, 198–214.
18 S. Van de Vyver, J. Geboers, P. A. Jacobs and B. F. Sels, *ChemCatChem*, 2011, **3**, 82–94.
19 I. T. Horváth, H. Mehdi, V. Fábos, L. Boda and L. T. Mika, *Green Chem.*, 2008, **10**, 238–242.
20 J. C. Serrano-Ruiz and J. A. Dumesic, *Energy Environ. Sci.*, 2011, **4**, 83–99.
21 W. R. H. Wright and R. Palkovits, *ChemSusChem*, 2012, **5**, 1657–1667.
22 J. Zhang, S. Wu, B. Li and H. Zhang, *ChemCatChem*, 2012, **4**, 1230–1237.
23 D. M. Alonso, S. G. Wettstein and J. A. Dumesic, *Green Chem.*, 2013, **15**, 584–595.
24 J. Q. Bond, D. M. Alonso, D. Wang, R. M. West and J. A. Dumesic, *Science*, 2010, **327**, 1110–1114.
25 J. P. Lange, R. Price, P. M. Ayoub, J. Louis, L. Petrus, L. Clarke and H. Gosselink, *Angew. Chem., Int. Ed.*, 2010, **49**, 4479–4483.
26 P. P. Upare, J. M. Lee, Y. K. Hwang, D. W. Hwang, J. H. Lee, S. B. Halligudi, J. S. Hwang and J. S. Chang, *ChemSusChem*, 2011, **4**, 1749–1752.
27 X.-L. Du, Q.-Y. Bi, Y.-M. Liu, Y. Cao, H.-Y. He and K.-N. Fan, *Green Chem.*, 2012, **14**, 935–939.
28 J. J. Bozell, *Science*, 2010, **329**, 522–523.
29 R. A. Bourne, J. G. Stevens, J. Ke and M. Poliakoff, *Chem. Commun.*, 2007, 4632–4634.
30 K. Yan, C. Jarvis, T. Lafleur, Y. Qiao and X. Xie, *RSC Adv.*, 2013, **3**, 25865–25871.
31 A. M. Hengne and C. V. Rode, *Green Chem.*, 2012, **14**, 1064–1072.
32 A. M. R. Galletti, C. Antonetti, V. De Luise and M. Martinelli, *Green Chem.*, 2012, **14**, 688–694.
33 S. G. Wettstein, J. Q. Bond, D. M. Alonso, H. N. Pham, A. K. Datye and J. A. Dumesic, *Appl. Catal., B*, 2012, **117**, 321–329.
34 W. Luo, U. Deka, A. M. Beale, E. R. van Eck, P. C. Bruijnincx and B. M. Weckhuysen, *J. Catal.*, 2013, **301**, 175–186.
35 R. A. W. Johnstone, A. H. Wilby and I. D. Entwistle, *Chem. Rev.*, 1985, **85**, 129–170.
36 L. Deng, J. Li, D. M. Lai, Y. Fu and Q. X. Guo, *Angew. Chem., Int. Ed.*, 2009, **48**, 6529–6532.
37 L. Deng, Y. Zhao, J. Li, Y. Fu, B. Liao and Q. X. Guo, *ChemSusChem*, 2010, **3**, 1172–1175.
38 X. L. Du, L. He, S. Zhao, Y. M. Liu, Y. Cao, H. Y. He and K. N. Fan, *Angew. Chem., Int. Ed.*, 2011, **50**, 7815–7819.
39 Z. Shen, Y. L. Zhang, F. M. Jin, X. F. Zhou, A. Kishita and K. Tohji, *Ind. Eng. Chem. Res.*, 2010, **49**, 6255–6259.
40 D. Kopetzki and M. Antonietti, *Green Chem.*, 2010, **12**, 656–660.
41 J. S. Cha, *Org. Process Res. Dev.*, 2006, **10**, 1032–1053.
42 G. K. Chuah, S. Jaenicke, Y. Z. Zhu and S. H. Liu, *Curr. Org. Chem.*, 2006, **10**, 1639–1654.
43 J. R. Ruiz and C. Jimenez-Sanchidrian, *Curr. Org. Chem.*, 2007, **11**, 1113–1125.
44 N. J. Wise and J. M. J. Williams, *Tetrahedron Lett.*, 2007, **48**, 3639–3641.
45 M. Chia and J. A. Dumesic, *Chem. Commun.*, 2011, **47**, 12233–12235.
46 R.-J. van Putten, J. C. van der Waal, E. de Jong, C. B. Rasrendra, H. J. Heeres and J. G. de Vries, *Chem. Rev.*, 2013, **113**, 1499–1597.
47 Y. Román-Leshkov, J. N. Chheda and J. A. Dumesic, *Science*, 2006, **312**, 1933–1937.
48 E. Nikolla, Y. Roman-Leshkov, M. Moliner and M. E. Davis, *ACS Catal.*, 2011, **1**, 408–410.
49 E. Creyghton, S. Ganeshie, R. Downing and H. Van Bekkum, *J. Mol. Catal. A: Chem.*, 1997, **115**, 457–472.
50 A. Corma, M. E. Domine, L. Nemeth and S. Valencia, *J. Am. Chem. Soc.*, 2002, **124**, 3194–3195.
51 A. Corma, M. E. Domine and S. Valencia, *J. Catal.*, 2003, **215**, 294–304.
52 Y. Zhu, G. K. Chuah and S. Jaenicke, *J. Catal.*, 2006, **241**, 25–33.
53 P. P. Samuel, S. Shylesh and A. P. Singh, *J. Mol. Catal. A: Chem.*, 2007, **266**, 11–20.
54 A. Ramanathan, M. C. Castro Villalobos, C. Kwakernaak, S. Telalovic and U. Hanefeld, *Chem.–Eur. J.*, 2008, **14**, 961–972.
55 G. Chuah and S. Jaenicke, *Appl. Catal., A*, 1997, **163**, 261–273.
56 P. S. Kumbhar, J. Sanchez-Valente, J. Lopez and F. Figueras, *Chem. Commun.*, 1998, 535–536.
57 S. Liu, S. Jaenicke and G. Chuah, *J. Catal.*, 2002, **206**, 321–330.
58 M. Kotani, T. Koike, K. Yamaguchi and N. Mizuno, *Green Chem.*, 2006, **8**, 735–741.
59 F. J. Urbano, M. A. Aramendia, A. Marinas and J. M. Marinas, *J. Catal.*, 2009, **268**, 79–88.
60 J. Ramos, V. Díez, C. Ferretti, P. Torresi, C. Apesteguía and J. Di Cosimo, *Catal. Today*, 2011, **172**, 41–47.
61 J. F. Miñambres, M. A. Aramendía, A. Marinas, J. M. Marinas and F. J. Urbano, *J. Mol. Catal. A: Chem.*, 2011, **338**, 121–129.
62 J. K. Bartley, C. Xu, R. Lloyd, D. I. Enache, D. W. Knight and G. J. Hutchings, *Appl. Catal., B*, 2012, **128**, 31–38.
63 T. Jyothi, T. Raja and B. Rao, *J. Mol. Catal. A: Chem.*, 2001, **168**, 187–191.
64 J. R. Ruiz, C. Jiménez-Sanchidrián and J. M. Hidalgo, *Catal. Commun.*, 2007, **8**, 1036–1040.

65 R. Radhakrishnan, D. M. Do, S. Jaenicke, Y. Sasson and G. K. Chuah, *ACS Catal.*, 2011, **1**, 1631–1636.
66 Y. Zhu, S. Jaenicke and G. Chuah, *J. Catal.*, 2003, **218**, 396–404.
67 Y. Nie, S. Jaenicke and G. K. Chuah, *Chem.–Eur. J.*, 2009, **15**, 1991–1999.
68 G. Yang, E. A. Pidko and E. J. M. Hensen, *J. Phys. Chem. C*, 2013, **117**, 3976–3986.
69 G. Guo and Y. Chen, *J. Mater. Sci.*, 2004, **39**, 4039–4043.
70 S. Axpuac, M. Aramendía, J. Hidalgo-Carrillo, A. Marinas, J. Marinas, V. Montes-Jiménez, F. Urbano and V. Borau, *Catal. Today*, 2012, **187**, 183–190.
71 E. Parry, *J. Catal.*, 1963, **2**, 371–379.
72 D. M. Bibby, R. F. Howe and G. D. Mclellan, *Appl. Catal., A*, 1992, **93**, 1–34.
73 J. Kim, M. Choi and R. Ryoo, *J. Catal.*, 2010, **269**, 219–228.
74 P. P. Upare, J.-M. Lee, D. W. Hwang, S. B. Halligudi, Y. K. Hwang and J.-S. Chang, *J. Ind. Eng. Chem.*, 2011, **17**, 287–292.
75 D. M. Alonso, S. G. Wettstein, J. Q. Bond, T. W. Root and J. A. Dumesic, *ChemSusChem*, 2011, **4**, 1078–1081.
76 E. I. Gurbuz, D. M. Alonso, J. Q. Bond and J. A. Dumesic, *ChemSusChem*, 2011, **4**, 357–361.